ICRIE 2023 4th INTERNATIONAL CONFERENCE ON RECENT INNOVATIONS IN ENGINEERING

Proceedings of the 4th International Conference on Recent Innovation in Engineering
ICRIE 2023, University of Duhok, College of Engineering, 13th – 14th September 2023
(Special issue for Passer journal of basic and applied sciences)
Paper No. 21

Tensor decomposition-based compression and noise reduction of multichannel ECG signals

THOMAS SCHANZE[1,*]

[1]Institute for Biomedical Engineering, Faculty of Life Science Engineering (LSE), Technische Hochschule Mittelhessen (THM) - University of Applied Sciences, Germany - E-mail: thomas.schanze@lse.thm.de

* Corresponding author: Institute for Biomedical Engineering, Faculty of Life Science Engineering (LSE), Technische Hochschule Mittelhessen (THM) - University of Applied Sciences, Germany. Tel: +49 641 309-2639.

ABSTRACT

The electrocardiogram (ECG) is an important diagnostic tool in medicine. During a recording, ECG waveforms may change due to intrinsic processes, changes in recording parameters, such as recording electrode properties, and especially artefacts, e.g., electromagnetic hum or noise. Clearly, signal distortion can adversely affect medical decisions. In recent years, a variety of signal processing methods have been introduced to remove noise from signals. One of these methods is singular value decomposition (SVD)-based denoising, in which QRS-aligned sections of a signal channel are arranged in a matrix, which is then decomposed into singular values and left and right singular vectors. However, the right combination of these components can result in surprisingly good noise reduction. For multichannel recordings, this approach can be applied to each single channel. This means that cross-channel correlations, i.e., signal correlations between channels, cannot be used. An obvious extension for the analysis of QRS-aligned multichannel signal sections is their representation by a three-dimensional array, i.e., a third-order tensor with the dimensions time, segment and channel. Here, we show how to denoise tensorized QRS-aligned multichannel ECG sections, each comprising P-wave, QRS-complex, and T-wave, by higher-order singular value decomposition (HOSVD). We present a method for combining HOSVD components for denoising, i.e., noise reduction. Furthermore, we show that not only noise reduction but also data compression can be achieved with this method. Denoising quality is evaluated by using the Pearson correlation coefficient and extended Frobenius norm calculated for noisy and original and also for denoised and original signals. Gaussian white noise was used for the contamination of the original multichannel recordings, resulting in test data with various signal-to-noise ratios. The compression ratio determines the compression performance. With the proposed method, the correlations between the noisy and the original signal and the denoised signal with the original signal could be increased significantly, e.g., from around 0.45 to 0.97, and this at a compression rate of around 127. However, the tensor decomposition-based noise reduction of multiple channels often yields better results than the SVD-based single-channel denoising. This is the case when there are correlations between the channels in the multichannel signal to be denoised, especially correlations in the wanted signals. A scenario with more realistic noise conditions was generated by using an ECG simulator to further analyze the properties of HOSVD-based compression and denoising. This led to the finding that the selection of the HOSVD computed reconstruction components required

for denoising needs to be done carefully. To conclude, tensor decomposition-based compression and denoising can be an appropriate tool for the compression and denoising of multichannel signals. However, its usefulness under real-world conditions has yet to be demonstrated.

Keywords: Biosignal; Compression; Denoising; Signal processing; Singular value decomposition; Tensor decomposition

1. INTRODUCTION

The introduction of chest X-rays in 1895 and the electrocardiogram (ECG) in 1902 provided objective and, most importantly, relevant information about the structure and function of the heart. (Howell, 1991). In the first half of the 20th century, a series of innovative discoveries and inventions led to the 12-lead ECG as we know it today. (Fye, 1994; AlGhatrif & Lindsay, 2012). ECG signals are one of the best-understood biomedical signals, and they provide important diagnostic information. Despite these successes, it is still important to improve or develop signal processing methods and procedures so that diagnostically relevant ECG features can be detected more effectively and reliably. Important features of an ECG are P-wave, QRS-complex, and T-wave: the P-wave indicates atrial depolarization, the QRS-complex reflects ventricular depolarization, and the T-wave represents ventricular repolarization. However, if no P-wave is present, there is a lack of atrial depolarization.

Unfortunately, the ECG is often corrupted by noise and artefacts (Limaye & Deshmukh, 2016; Kher, 2019). Typical ECG contaminants are patient-electrode motion artefacts, electrode noise and pop artefacts, powerline interference, electromyographic noise, baseline wandering noise, electrosurgical noise, and noise of the data acquisition device. If the amplitude of a perturbation is in the range of the desired signal and if, in addition, the perturbation and desired signal spectrally overlap, then this generally results in a significant impairment of the time course or the quality of the desired signal.

Noise suppression methods aim to remove unwanted noise and, of course, artefacts from a signal in such a way that the wanted signal is not changed as much as possible. This is especially difficult if the useful or wanted signal is not well known.

Signal denoising is a problem that has been studied for many years. However, it remains a challenging and open task. The main reason for this is that, from a mathematical point of view, signal denoising is an inverse problem whose solution is often ambiguous. Nevertheless, signal denoising has achieved great success in the last decades and a variety of methods, which also comprise machine learning, have been developed (Ardeti et al., 2023; Chatterjee et al., 2020; Fan et al., 2019; Halidou et al., 2023; Maghfiroh et al., 2022; Samann & Schanze, 2021; Samann & Schanze, 2023; Schanze, 2018).

The main goal of lossless data or signal compression techniques is to eliminate redundancies but not to change the information content (Elgendi et al., 2019; Jalaleddine et al., 1990; Jayasankar et al., 2021; Salomon, 2007;). However, lossy signal compression is related to signal denoising in that both approaches aim to filter out the irrelevant content and retain only the relevant or wanted signal components or features. Thus, lossy compression and denoising are information reduction methods.

Many lossy compression but also denoising techniques consist of two complementary processing steps: decomposition and reconstruction. Classically, the decomposition is performed by means of predefined functions, e.g., sinusoidal waves or wavelets. In more recent methods, the basis for the representation of the data is calculated from the data itself. Some of these methods use singular vector decomposition (Gong et al., 2017; Ouali & Chafaa, 2013; Schanze, 2018; Schanze, 2022; Wei et al., 2001). Such a method is singular spectrum analysis (SSA), which may also be used for prediction (Golyandina & Zhigljavsky, 2020; Sanei & Hassani, 2016). However, SSA works for single-channel signals. In SSA, the first decomposition step is the two-dimensional embedding of a one-dimensional data structure. If a vector can represent the time series, then it is mapped into a Hankel or, what is equivalent, into a Toeplitz matrix. If the embedding is done into a Hankel matrix, then this is also called Hankelisation (Schanze, 2018).

The next decomposition step is to decompose the Hankel matrix by singular value decomposition (SVD) into a sum of singular value weighted rank-one matrices, which are outer products of the related

left and right singular vectors. The reconstruction of the wanted signal can be achieved by an expedient modification or adjustment of the weights, which yields an approximated Hankel matrix, and by the appropriate back transformation. However, compared to classical linear filtering approaches, e.g., by aperiodic or Bessel bandpass filters, the structure of the desired time series is often less affected by SSA-denoising. The extension to multichannel signals was recently developed (Schanze, 2023b).

Another approach to noise reduction of the ECG is single-channel noise reduction. Here, an ECG channel is partitioned into QRS-aligned segments, where each segment may contain the P- and T-waves associated with the QRS complex. (Schanze, 2022). These segments can be combined into a two-dimensional data structure, i.e., a matrix. SVD can decompose this matrix into a set of rank-one matrices. A smart selection in conjunction with a subsequent superimposition of these matrices can lead to segments with high-quality denoising. The extension to multichannel signals was recently developed (Schanze, 2023a).

Many data sets consist of two-dimensional data. Examples include images and multivariate time series. An important biomedical signal is the standard 12-lead ECG signal. Due to its structure, the 12-lead ECG signal can be considered as a two-dimensional data set with the dimensions of time and channel.

When analyzing the channels of a multivariate time series individually, correlations between the channels are not taken into account. To overcome this drawback, we rely in this work on a method that was developed for compression of QRS-aligned segments of multichannel ECG (Schanze, 2023a).

The goal of this paper is to show that tensor decomposition-based compression and noise reduction can be a useful tool for processing multichannel signals, e.g., 12-lead ECG.

The paper proceeds as follows. In the Methods section the SVD-based decomposition of matrices is shortly reviewed. Then, based on the SVD, the decomposition and approximation of tensors is presented. We then describe the denoising of QRS-aligned segments of a single-channel ECG signal. Thereupon, relying on the compression of QRS-aligned segments of a multichannel ECG, a method for denoising such segments is introduced. In the Results section, artificially noisy signals are used to demonstrate the performance of tensor decomposition-based compression and noise reduction. SVD-based denoising is used as a reference. The paper ends with a discussion and conclusions section.

2. METHODS

2.1 Singular Value Decomposition

Singular value decomposition (SVD) is an important mathematical tool. For a synopsis of the early history of SVD see Steward (1993). We provide here a brief, incomplete overview. Let $\mathbf{A}$ be an $m \times n$ matrix. The SVD of $\mathbf{A}$ yields three matrices that satisfy the following equation:

$$\mathbf{A} = \mathbf{U}\,\mathbf{S}\,\mathbf{V}^{\mathrm{T}} \qquad (1),$$

where $\mathbf{U}$ is an orthogonal $m \times m$ matrix, $\mathbf{S}$ is a diagonal $m \times n$ matrix with ordered non-negative entries, i.e., $s_{i,i} \geq s_{i+1,i+1} \geq 0$, and $\mathbf{V}$ is an orthogonal $n \times n$ matrix. The $s_{i,i}$ are named as singular values, and the columns of $\mathbf{U}$ and $\mathbf{V}$ are referred to as left and right singular vectors (Andrews & Patterson, 1976; Golub & Reinsch 1970; Jain, 1981; Mac Duffee, 1933; Steward, 1993). When $\mathbf{A}$ has full rank, i.e., $r = \mathrm{rank}(\mathbf{A}) = \min(m, n)$, then all singular values are larger than zero.

It is well known that (1) can be rewritten:

$$\mathbf{A} = \sum_{i=1}^{r} \mathbf{A}_i = \sum_{i=1}^{r} s_{i,i}\,\mathbf{u}_i \otimes \mathbf{v}_i \qquad (2).$$

Note, the outer product $\mathbf{u}_i \otimes \mathbf{v}_i$ is normalized: $\|\mathbf{u}_i \otimes \mathbf{v}_i\| = 1$. Thus, $s_{i,i}$ is associated with the meaning of $\mathbf{u}_i \otimes \mathbf{v}_i$ in the representation of $\mathbf{A}$: the larger an $s_{i,i}$, the greater its importance. However, this property is important for compression and denoising. It should also be mentioned that $\mathrm{rank}(\mathbf{A}_i) = 1$ and that the singular values are said to make up the singular value spectrum.

2.2 Third-order Tensor Decomposition

Simplified, a tensor decomposition is a scheme for representing a tensor as a sequence of operations acting on other, often simpler tensors (Kolda and Bader, 2009; Liu, 2021; Wrede, 1972). Thus, SVD is a special tensor decomposition: since a matrix is a tensor of order two, SVD is a second-order tensor decomposition. Note that SVD and related higher-order tensor decompositions are multilinear.

A rather simple but intuitive approach to tensors is to consider them as higher-order data structures. A matrix is a two-dimensional data structure. Examples are images or data vectors arranged as a matrix. A movie, which is a sequence of images, can be thought of as a third-order tensor. Another example is a time-segmented 12-lead ECG. Here, we have the dimensions of time, channel, and segment (epoch). Accordingly, one can also imagine higher-dimensional data structures, i.e., higher-order tensors. The goal of a higher-order tensor decomposition is, as mentioned, to represent a tensor by a sequence of operations acting on tensors of equal or lower order. However, higher-order tensors can often be decomposed in several ways. One approach is higher-order SVD. In the following, we will restrict ourselves to a decomposition procedure for tensors of order three, i.e., third-order SVD.

Let $\mathbf{A}$ be an $(m \times n \times o)$ tensor. Thus, an element of $\mathbf{A}$ is indexed by three variables, i.e., $a_{i,j,k}$, $i = 1, 2, \dots, m$, $j = 1, 2, \dots, n$, and $k = 1, 2, \dots, o$. It is now the case that this tensor can be represented as follows:

$$\mathbf{A} = \sum_{i=1}^{m} \sum_{j=1}^{n} \sum_{k=1}^{o} \mathbf{A}_{i,j,k} = \sum_{i=1}^{m} \sum_{j=1}^{n} \sum_{k=1}^{o} s_{i,j,k}\, \mathbf{u}_i \otimes \mathbf{v}_j \otimes \mathbf{w}_k \qquad (3),$$

where $s_{i,j,k}$ is an element of the so-called core-tensor $\mathbf{S}$ (see Schanze, 2023a). It is easy to verify that this is a tensor of order three. The vectors $\mathbf{u}_i$, $\mathbf{v}_j$, and $\mathbf{w}_k$ are column vectors, which are linked together via outer products to form tensors. These vectors can be combined to matrices, i.e., $(m \times m)$ matrix $\mathbf{U}$, $(n \times n)$matrix $\mathbf{V}$, and $(o \times o)$ matrix $\mathbf{W}$. The process of computing $\mathbf{S}$, $\mathbf{U}$, $\mathbf{V}$, and $\mathbf{W}$, given $\mathbf{A}$, is called third-order singular value decomposition (Kolda & Bader, 2009; Liu, 2021). Figure 1 shows an illustration of a third-order tensor decomposition by third-order SVD.

2.3 A Straightforward Approximation of a Third-order Tensor

We now look at $s_{i,j,k}\, \mathbf{u}_i \otimes \mathbf{v}_j \otimes \mathbf{w}_k$, cf. equation (3). This expression can be decomposed (Schanze, 2023a; Schanze, 2023b) into two parts: $s_{i,j,k}$ and $\mathbf{T}_{i,j,k} = \mathbf{u}_i \otimes \mathbf{v}_j \otimes \mathbf{w}_k$. However, $\mathbf{T}_{i,j,k}$ is an $(m \times n \times o)$ tensor. Let $t_{\alpha,\beta,\gamma}^{(i,j,k)}$ be an element of $\mathbf{T}_{i,j,k}$. If we define the extended Frobenius norm by

$$\left\|\mathbf{T}_{i,j,k}\right\|_{\mathrm{F}} = \sqrt{\sum_{\alpha=1}^{m} \sum_{\beta=1}^{n} \sum_{\gamma=1}^{o} \left[t_{\alpha,\beta,\gamma}^{(i,j,k)}\right]^2} \qquad (4),$$

then $\left\|\mathbf{T}_{i,j,k}\right\|_{\mathrm{F}} = 1$ holds. Since $s_{i,j,k}$ can also be negative, we consider its absolute value. As a result, $\left|s_{i,j,k}\right|$ may be interpreted as the importance of $\mathbf{T}_{i,j,k} = \mathbf{u}_i \otimes \mathbf{v}_j \otimes \mathbf{w}_k$ with respect to a representation of $\mathbf{A}$ by (3). Thus, an approximation of $\mathbf{A}$ can be obtained by setting $s_{i,j,k} = 0$ to exclude unwanted $\mathbf{T}_{i,j,k}$ from (4). A somehow more useful alternative is to select those $\mathbf{A}_{i,j,k} = s_{i,j,k}\mathbf{T}_{i,j,k}$ that are appropriate for the approximation of $\mathbf{A}$.

Following Schanze (2023b), suppose that $\varphi_i(l)$, $\varphi_j(l)$, and $\varphi_k(l)$, $l = 1,2, \dots, d$, are mappings, which select the d most interesting $\mathbf{A}_{i,j,k}$. If such mappings are found, then

$$\mathbf{A}_{(d)} = \sum_{l=1}^{d} s_{\varphi_i(l),\varphi_j(l),\varphi_k(l)}\, \mathbf{u}_{\varphi_i(l)} \otimes \mathbf{v}_{\varphi_j(l)} \otimes \mathbf{w}_{\varphi_k(l)} \qquad (5)$$

is the desired approximation or lossy reconstruction. This approximation can be used for both compression and denoising. A straight forward selection is to choose those core-tensor elements with the highest absolute values.

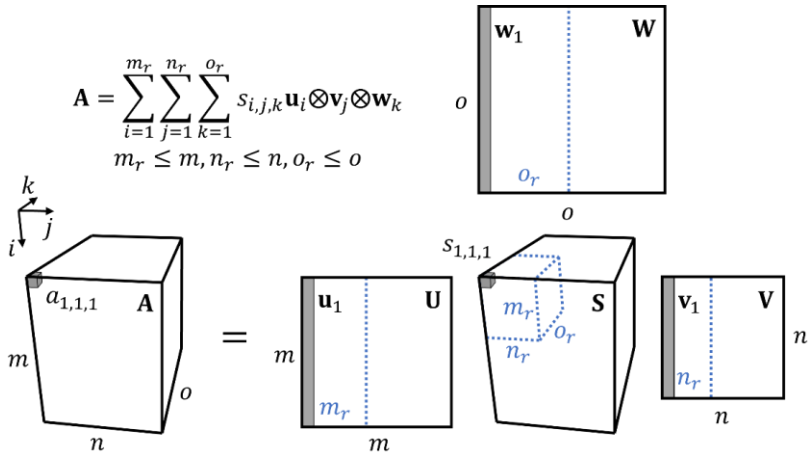

Figure 1. Illustration of the third-order SVD.

The $(m \times n \times o)$ tensors $\mathbf{S}$ and $\mathbf{A}$ are represented as cuboids, the matrices $\mathbf{U}$, $\mathbf{V}$, and $\mathbf{W}$ as rectangles. $a_{1,1,1}$ is the first element of $\mathbf{A}$, it is represented by a small grey cuboid in the upper left of $\mathbf{A}$ (lower left). The components of the expression $\mathbf{A}_{1,1,1} = s_{1,1,1}\, \mathbf{u}_1 \otimes \mathbf{v}_1 \otimes \mathbf{w}_1$, which are scalar and three-column vectors, are illustrated as grey objects in the drawings related to $\mathbf{S}$, $\mathbf{U}$, $\mathbf{V}$, and $\mathbf{W}$ (bottom right). However, $\mathbf{A}_{1,1,1}$ is also an $(m \times n \times o)$ tensor. The r-indexed markers indicate the structure for a subset. The regions associated with the r-indexed expressions indicate the structure for a subset. The formula on the top left shows the associated simple approximation approach based only on these bounds.

2.4 Compression and Denoising Quality Assessment

The data compression ratio can be defined as the ratio between the uncompressed and compressed size of the data to be analyzed. We restrict ourselves to third-order tensors, from which the corresponding calculations for third-order SVD-based compression or denoising can be easily derived.

Let $\mathbf{A}_{(d)}$ be an approximation of $\mathbf{A}$. For simplicity we assume that $\mathbf{A}$, $s_{\varphi_i(l),\varphi_j(l),\varphi_k(l)}$, $\mathbf{u}_{\varphi_i(l)}$, $\mathbf{v}_{\varphi_j(l)}$ and $\mathbf{w}_{\varphi_k(l)}$ are stored identically, e.g., by using double-precision floating-point format. It is easy to verify that the number of elements of $\mathbf{A}$ to be stored is

$$\#(\mathbf{A}) = m\, n\, o \qquad (6),$$

here the number of elements to store $\mathbf{A}_{(d)}$ is

$$\#\left(\mathbf{A}_{(d)}\right) = 4d_s + d_{\mathbf{u}} m + d_{\mathbf{v}} n + d_{\mathbf{w}} o \qquad (7),$$

where d_s is the number of the $s_{\varphi_i(l),\varphi_j(l),\varphi_k(l)}$ and where $d_{\mathbf{u}}$, $d_{\mathbf{v}}$, and $d_{\mathbf{w}}$ are each the number of the $\mathbf{u}_{\varphi_i(l)}$, $\mathbf{v}_{\varphi_j(l)}$, and $\mathbf{w}_{\varphi_k(l)}$, respectively, required to compute $\mathbf{A}_{(d)}$. The term $4d_s$ is due to the fact, that also indices must be stored. Thus the compression ratio is

$$CR = \#(\mathbf{A}) / \#\left(\mathbf{A}_{(d)}\right) = (m\, n\, o) / (4d_s + d_{\mathbf{u}} m + d_{\mathbf{v}} n + d_{\mathbf{w}} o) \qquad (8).$$

Please note, that it was taken into account that some vectors $\mathbf{u}_{\varphi_i(l)}$, $\mathbf{v}_{\varphi_j(l)}$ and $\mathbf{w}_{\varphi_k(l)}$ can be used more than once to approximate $\mathbf{A}$, which requires storing of additional data, i.e., indices. The numbers of the vectors used to compute $\#\left(\mathbf{A}_{(d)}\right)$ are

$$\#(\text{vec}) = (d_{\mathbf{u}}, d_{\mathbf{v}}, d_{\mathbf{w}}) \qquad (9).$$

In the case of SVD we find, by using equation (2)

$$\#\left(\mathbf{A}_{(d)}\right) = r(1 + m + n) \qquad (10).$$

Let $\mathbf{A}$ be a tensor, then the extended Frobenius norm $\|\mathbf{A}\|_{\mathrm{F}}$ is the square root of the sum of the absolute squares of the elements of $\mathbf{A}$. Given $\mathbf{A}_{(d)}$ and $\mathbf{A}$, we can introduce the distance measure via the extended Frobenius norm or, better, the Frobenius distance:

$$\mathrm{dist}_{\mathrm{F}}(\mathbf{A}_{(d)}, \mathbf{A}) = \left\|\mathbf{A}_{(d)} - \mathbf{A}\right\|_{\mathrm{F}} \quad (11).$$

Another distance measure can be defined by using the Pearson correlation coefficient. For this we suppose to define a mapping that maps $\mathbf{A}_{(d)}$ and $\mathbf{A}$ to vectors, i.e., $\mathbf{x} = \mathrm{vec}(\mathbf{A}_{(d)})$ and $\mathbf{y} = \mathrm{vec}(\mathbf{A})$. Then, we can compute

$$\rho_{\mathbf{x},\mathbf{y}} = \mathrm{cov}(\mathbf{x}, \mathbf{y})/(\sigma_{\mathbf{x}}\sigma_{\mathbf{y}}) \quad (12).$$

Both measures can be easily modified for SVD-based compression or denoising and for comparisons of higher-order tensors.

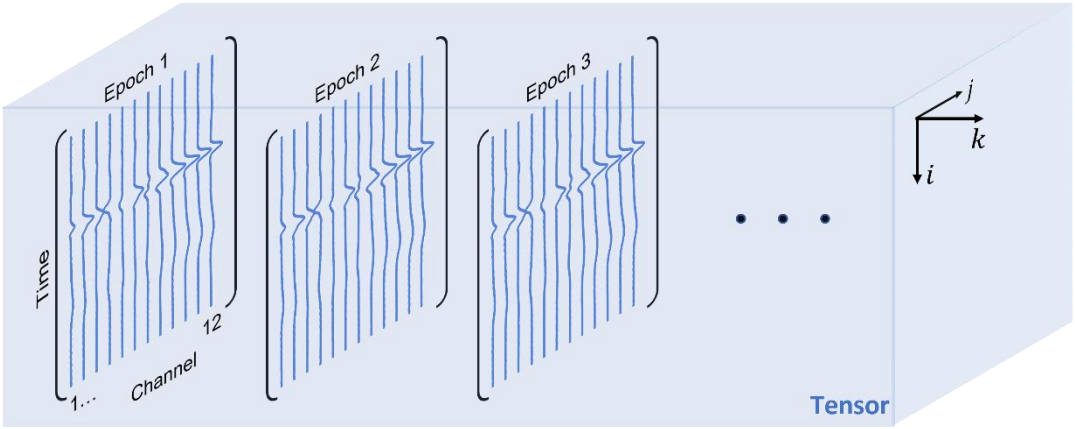

Figure 2. Combining QRS-aligned 12-lead ECG segments to a tensor.

The dimensions of the tensor are time, channel (lead), and epoch (heartbeat segment). The tensor contains a sequence of matrices, each of which contains QRS-aligned leads. P-waves, QRS-complexes and T-waves of an epoch belong to the same heartbeat. Note that the 12-lead ECG segments for each epoch can be represented by a matrix (brackets) and that these matrices are combined into a third-order tensor.

2.5 Tensorization, Algorithm and Programming

The main steps for compression or denoising of multidimensional ECG signals using QRS-based segmentation and tensor decomposition are:

1. QRS-detection, e.g., by using lead II
2. Generation of QRS-aligned segments (see Figure 2)
3. Tensorization: combining the segments to a tensor, as shown in Figure 2
4. Third-order tensor decomposition
5. Selection of wanted components for compression/denoising
6. Computation of the tensor approximation

Programming was done with Matlab R2022b and a tensor toolbox (Baader et al., 2022) for various types of tensor decomposition, especially for higher-order singular value decomposition. For QRS alignment, we used the Matlab function “findpeaks” with an appropriate threshold.

2.6 Signals and Testing

To demonstrate the performance of the presented tensor decomposition-based approach for compression and denoising, a database (Liu et al., 2018) consisting of classified 12-lead ECG recordings was selected. The data set with the number 281 was recorded from a healthy subject. It was chosen as an example and then segmented according to the location of the QRS complexes, i.e., the 12-channel data set was subdivided according to heartbeats. For this purpose, the QRS complexes of lead II were detected. Depending on the respective points in time, the channels were segmented in such a way that a three-dimensional data set with the dimensions time, channel and segment, i.e. epoch, was

created. Note that segmentation was performed so that all segments contain interrelated P-waves, QRS-complexes, and T-waves, each aligned to the respective point in time of QRS-complex of the lead II. All segments were thus aligned phase-locked according to the respective lead II QRS-complexes in the same way and with identical lengths. As a result, a three-dimensional data structure, i.e., a tensor, was created. Figure 2 illustrates such a tensor. We want to mention that the signals were bandpass filtered, 0.1 to 100 Hz, and sampled at 500 Hz. Each segment has a length of $m = 401$ data points, the number of channels is $n = 12$, and the number of segments or epochs per channel is $o = 34$; thus the total number of data points is $m\,n\,o = 163{,}608$.

Independent Gaussian white noise (GWN) was added to each segment to test compression and denoising. In addition, the standard deviation of the noise was varied. Compression ratio, Frobenius distance and Pearson correlation coefficient have been selected to assess the quality of SVD- and third-order SVD-based compression and denoising of QRS-aligned segments.

Note that this simple noise corruption approach ignores Einthoven's law, i.e., lead I + lead III = lead II. However, this is not critical as taking this law into account would have made compression easier due to lead dependency, but, also, depending on the noise type, denoising could be more difficult when correlations between channels must be taken into account to separate wanted signal and noise. In particular, against the background that, when denoising, representatives for the wanted signal and noise that are as separate as possible must be found, whereas when compressing, the most effective representation possible must be identified.

However, all ECG recordings in the database used (Liu et al., 2018) unfortunately only have a very limited number of heartbeats per signal set, which limits an examination of low-frequency artefacts or noise components such as baseline wander, which can also be correlated across channels.

To overcome this restriction, we used the Matlab version of an ECG simulation tool (Sološenko et al., 2021). We simulated a pure sinoatrial node-driven 12-lead ECG with 1,000 heartbeats and a related data set containing a mixture of muscle noise, electrode movement artefacts and baseline wander. We chose such a combination of interfering signals because they often occur in real ECG recordings. To create a noisy ECG, the original simulated ECG and the simulated noise were superimposed. The sampling rate was set to 1,000 Hz, and a signal-to-noise ratio of $\sigma_S/\sigma_N = 0.5$ was selected. Each segment has a length of $m = 801$ data points. For ECG segmentation the QRS detection and alignment and procedure described above were applied. The denoising of these multidimensional ECG segments was performed according to the above-introduced tensor decomposition-based method.

3. RESULTS

To demonstrate the performance of the method, different signal-to-noise ratios, each calculated over the full associated signal sets, were chosen: $S/N = \infty, 2, 1, 1/2$. Figure 3 shows the fifth segment of the original, the noisy and the denoised 12-lead ECG, depending on the S/N. The value $S/N = \infty$ was selected to show the pure signal compression quality. The six largest core-tensor elements in terms of magnitude were chosen, i.e., $d_s = 6$. Table 1 summarizes the results for the measures defined above, i.e., Pearson correlation coefficient, Frobenius distance, number of vectors used to compute the approximation, and the compression ratio. Please convince yourself that the respective used tensor decomposition components are dataset-dependent, which is shown by the vector selection $\#(\mathrm{vec})$ for a fixed number of core-tensor elements d_s. Note, that the sets obtained $d_s = 6$ can be a superset of the sets obtainable for $d_s < 6$. Note, a set means interrelated elements of the core-tensor $\mathbf{S}$ and the matrices $\mathbf{U}$, $\mathbf{V}$, and $\mathbf{W}$. Table 1 also shows the results for $d_s = 3$. We would like to point out that for no or weak noise, denoising for $d_s > 3$ is better than for $d_s = 3$. On the other hand, for strong noise, it is sufficient to denoise only for $d_s = 3$. From Figure 3 and Table 1, it follows that tensor decomposition-based compression or denoising clearly reconstructs the original signal waveforms while removing Gaussian white noise remarkably well. The high compression ratios also show that the method not only effectively denoises but is also suitable for efficient storage of ECG.

A double-logarithmic plot of the absolute values of the core-tensor elements, sorted in descending order, i.e., $s_{\varphi_i(l),\varphi_j(l),\varphi_k(l)} \geq s_{\varphi_i(l+1),\varphi_j(l+1),\varphi_k(l+1)}$, obtained for a signal-to-noise ratio of $\sigma_S/\sigma_N = 0.5$, is shown in Figure 4. Please note that the first values are many times larger than the last values. In addition, the first values are mainly related to ECG components, the rest to noise. Using the Scree plot (Schanze, 2023b), the number of core elements required for denoising was estimated to be three.

As mentioned earlier, another approach to ECG noise reduction is single-channel noise reduction by using SVD. We followed the procedure given by Schanze (2022) for lead II. Thus, the 34 QRS-aligned segments of lead II of the data set used for tensor-based denoising were used. Figure 5 shows the comparison of SVD and third-order SVD-based denoising. For SVD-based denoising, only the first singular value and the first left and right singular vectors were used. Note that this led to the best result. For third-order SVD-based denoising, which is a special third-order tensor decomposition-based denoising, $d_s = 3$ was used. The signal-to-noise ratio is $\sigma_S/\sigma_N = 1/2$ (all segments). Table 2 shows the corresponding results for the measures defined above, especially that third-order SVD-based denoising outperforms SVD-based denoising.

For the simulated ECG superimposed with more realistic interferences, i.e., a mixture of muscle noise, electrode movement artefacts and baseline wander, we found that a simple selection of core-tensor elements and the related components is generally not appropriate for high-quality denoising. Simple selection means here to select approximation or denoising components based on a scree plot of the absolute values of the core-tensor elements only (cf. Figure 4).

We would like to illustrate this with an example obtained for a 12-lead ECG with an overall signal-to-noise ratio of $\sigma_S/\sigma_N = 0.5$. Table 3 shows the noise improvements achieved as a function of the components selected for the three largest core-tensor elements for denoising. The core-tensor elements, sorted in absolute value descending order, are as follows: $s_{1,1,1}$, $s_{2,2,1}$, and $s_{1,3,2}$. Thus $s_{1,1,1}\,\mathbf{u}_1 \otimes \mathbf{v}_1 \otimes \mathbf{w}_1 + s_{2,2,1}\,\mathbf{u}_2 \otimes \mathbf{v}_2 \otimes \mathbf{w}_1 + s_{1,3,2}\,\mathbf{u}_1 \otimes \mathbf{v}_3 \otimes \mathbf{w}_2$ is the approximation or denoised version of all noisy segments. If the core-tensor element $s_{1,3,2}$ is exchanged against $s_{3,1,1}$, which has the seventh largest absolute value, then we have to compute $s_{1,1,1}\,\mathbf{u}_1 \otimes \mathbf{v}_1 \otimes \mathbf{w}_1 + s_{2,2,1}\,\mathbf{u}_2 \otimes \mathbf{v}_2 \otimes \mathbf{w}_1 + s_{3,1,1}\,\mathbf{u}_3 \otimes \mathbf{v}_3 \otimes \mathbf{w}_1$ to get denoised segments. Based on the values for correlation and extended Frobenius distance of Table 3, it follows that the second approximation or denoising is significantly better than the first. This shows that the choice of elements for approximation or denoising should be carried out carefully.

Figure 6 shows 20 consecutive Wilson V4 segments of the simulated 12-lead ECG, as well as the corresponding noisy and denoised segments. Recall that to generate the noisy signal, a mixture of muscle noise, electrode motion artefacts, and baseline wander was superimposed on the simulated ECG, also shown in Figure 6. The denoising was achieved by means of $s_{1,1,1}\,\mathbf{u}_1 \otimes \mathbf{v}_1 \otimes \mathbf{w}_1 + s_{2,2,1}\,\mathbf{u}_2 \otimes \mathbf{v}_2 \otimes \mathbf{w}_1 + s_{3,1,1}\,\mathbf{u}_3 \otimes \mathbf{v}_3 \otimes \mathbf{w}_1$. The excellent noise reduction of high-frequency components can be seen very clearly, while the low-frequency component, which essentially belongs to the baseline wandering noise, influences the amplitudes of the P-wave, QRS-complexes and T-waves. A reason for this is that some $\mathbf{u}_i$ represent both ECG and noise components.

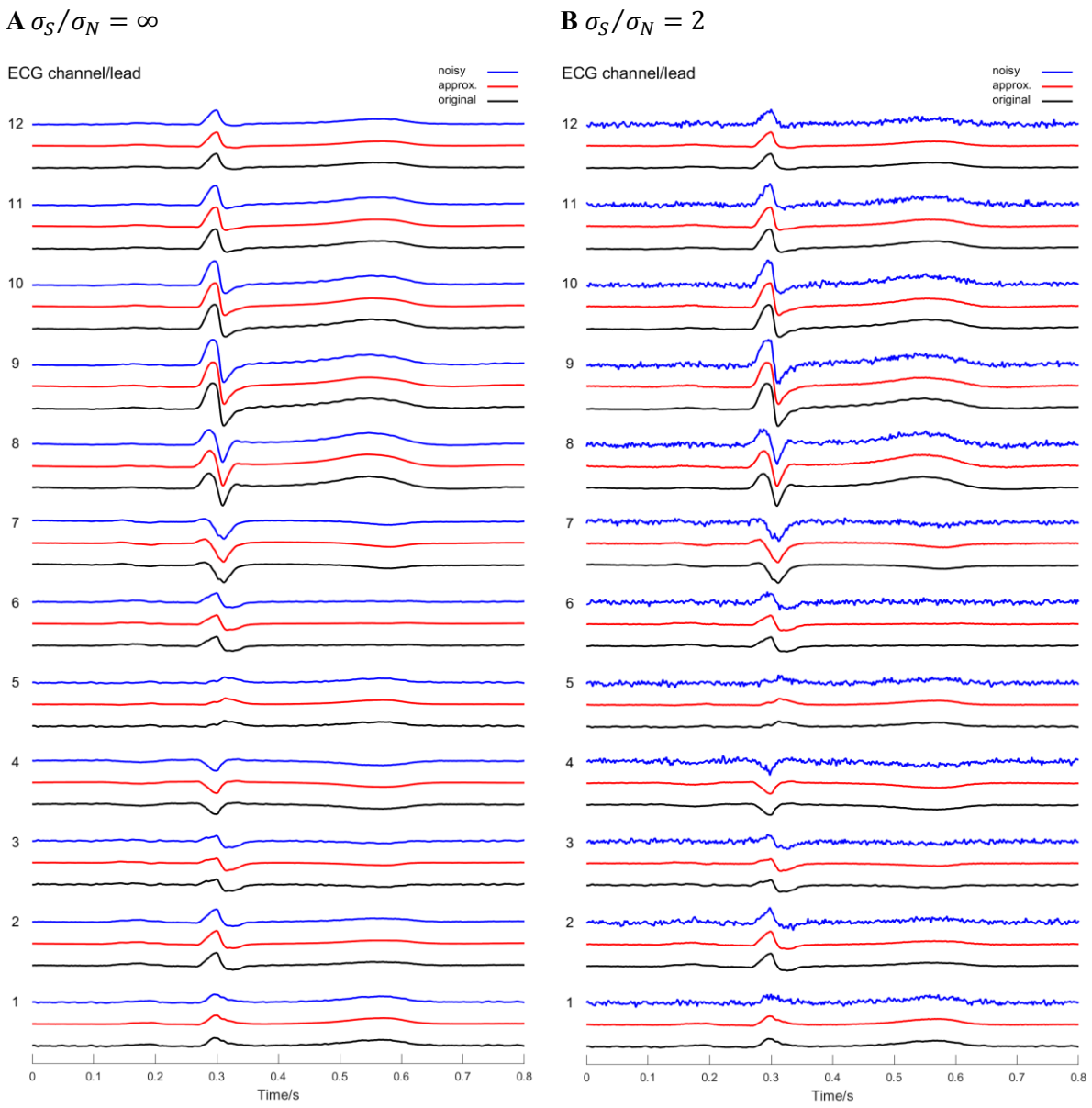

Figure 3. Compression and denoising of a 12-lead ECG for various signal-to-noise ratios.

Each subfigure (A-D) contains 12 groups, which are in relation to the ECG leads. Each group consists of 3 signals: black: original signal, red: approximated or denoised signal, and blue: original signal with Gaussian white noise (GWN) overlay. Shown is the fifth epoch (segment) of in total 34 epochs used for tensor decomposition-based compression/denoising. Please note that the GWN, which was statistically independently superimposed on all segments to generate noisy segments, could be reduced significantly. However, the larger the amplitude of a P-wave, a QRS-complex or a T-wave, the better the respective waveform of the denoised signal matches the original waveform. Furthermore, this property is quite independent of the signal-to-noise ratio. The compression ratio is 62.6, which indicates effective compression. It is to be noted that in A, the approximated signals contain fewer ripples than the original signals because the approximation, i.e., the compression, is lossy.

C $\sigma_S/\sigma_N = 1$ **D** $\sigma_S/\sigma_N = 0.5$

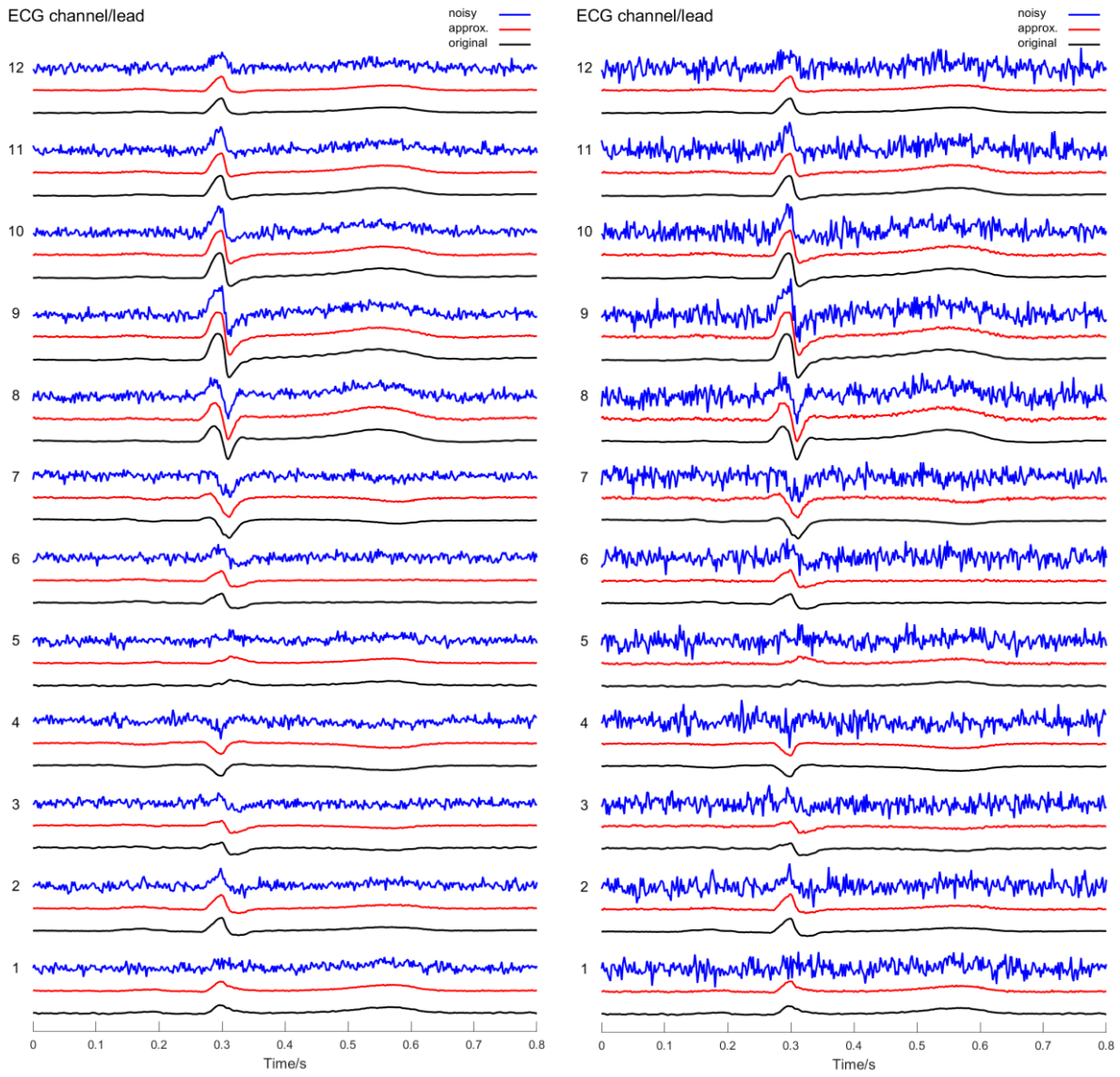

Continuation of **Figure 3.**

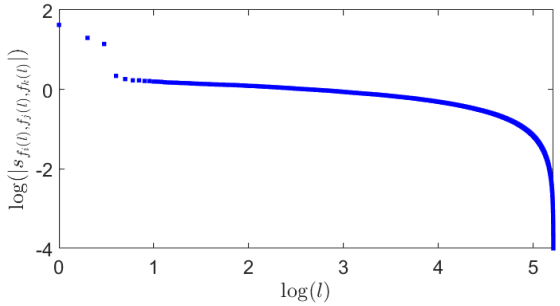

Figure 4. In descending order sorted absolute values of core-tensor elements for a signal-to-noise ratio $\sigma_S/\sigma_N = 0.5$.

Due to the structure of this graph, which can also be interpreted as a scree plot, the number of core-tensor elements required for denoising was estimated to be three. Please note the double logarithmic representation.

Table 1. Third-order SVD-based denoising quality. Pearson correlation coefficient ρ and Frobenius distance $\mathrm{dist_F}$ as a function of signal-to-noise ratio: σ_S/σ_N. Original signal: S, Gaussian white noise (GWN): N, noisy signal: $S+N$, denoised signal: $\mathrm{den}(S+N)$. These measures were applied to vectorized data (see section 2.4). The number of core-tensor elements which have been selected for approximation by equation (5) is given by d_s, #(vec) denotes the numbers of the vectors used to compute the approximation, and CR is the compression ratio. Note that a GWN was created for each segment and, for ease of comparison, only the standard deviation was scaled for each segment according to the specifications.

d_s	σ_S/σ_N	$\rho_{S,S+N}$	$\rho_{S,\mathrm{den}(S+N)}$	$\mathrm{dist_F}(S,S+N)$	$\mathrm{dist_F}(S,\mathrm{den}(S+N))$	#(vec)	CR
6	∞	1	0.993	0	5.9	(6, 4, 3)	63.4
6	2	0.894	0.991	24.2	6.5	(6, 4, 3)	63.4
6	1	0.707	0.986	48.4	8.0	(5, 5, 2)	75.8
6	0.5	0.447	0.970	96.9	12.0	(6, 4, 4)	62.6
3	∞	1	0.989	0	7.4	(3, 3, 1)	127.3
3	2	0.894	0.986	24.2	7.6	(3, 3, 1)	127.3
3	1	0.707	0.985	48.4	8.5	(3, 3, 1)	127.3
3	0.5	0.447	0.971	96.9	11.6	(3, 3, 1)	127.3

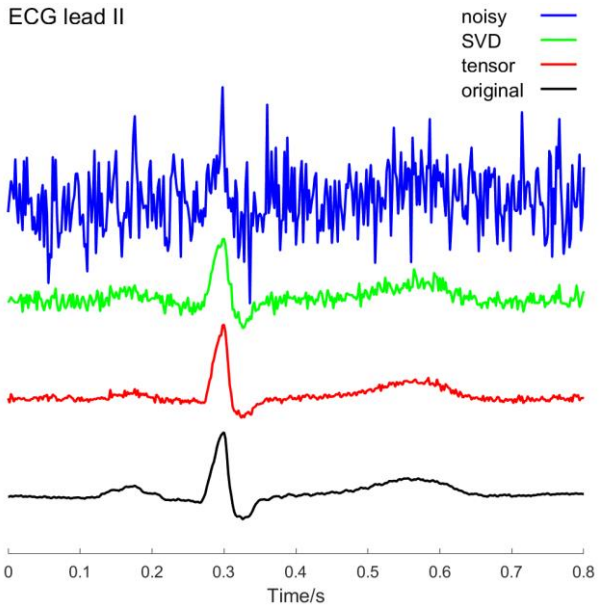

Figure 5. Denoising quality for single-channel SVD and for multichannel third-order SVD-based denoising of a 12-lead ECG. Note, only lead II was used for SVD-based ECG denoising. The fifth segment out of 34 segments is shown for original signal (black), noisy signal (blue), SVD-based denoised signal (green) and third-order SVD-based denoised signal (tensor, red).

Table 2. Denoising quality for single-channel SVD and for multichannel third-order SVD-based denoising of a 12-lead ECG. Note, only lead II was used for classical SVD-based ECG denoising. Pearson coefficient ρ and Frobenius distance $\mathrm{dist_F}$ as a function of signal-to-noise ratio: σ_S/σ_N. Original signal: S, Gaussian white noise: N, noisy signal: $S+N$, denoised signal: $\mathrm{den}(S+N)$.

Denoising type	$\rho_{S,S+N}$	$\rho_{S,\mathrm{den}(S+N)}$	$\mathrm{dist_F}(S,S+N)$	$\mathrm{dist_F}\big(S,\mathrm{den}(S+N)\big)$
SVD	0.349	0.889	28.0	5.6
Third-order SVD		0.965		2.7

Table 3. Denoising quality for multichannel third-order SVD-based denoising of a simulated 12-lead ECG depends on the selection of the core-tensor elements, i.e., elements that were not set to zero for the approximation or denoising. The overall signal-to-noise ratio is $\sigma_S/\sigma_N = 0.5$. The notations are based on those of Table 1 or 2.

Core-tensor elements	$\rho_{S,S+N}$	$\rho_{S,\mathrm{den}(S+N)}$	$\mathrm{dist_F}(S,S+N)$	$\mathrm{dist_F}\big(S,\mathrm{den}(S+N)\big)$
$s_{1,1,1}$, $s_{2,2,1}$, $s_{1,3,2}$	0.848	0.930	274	166
$s_{1,1,1}$, $s_{2,2,1}$, $s_{3,1,1}$		0.971		106

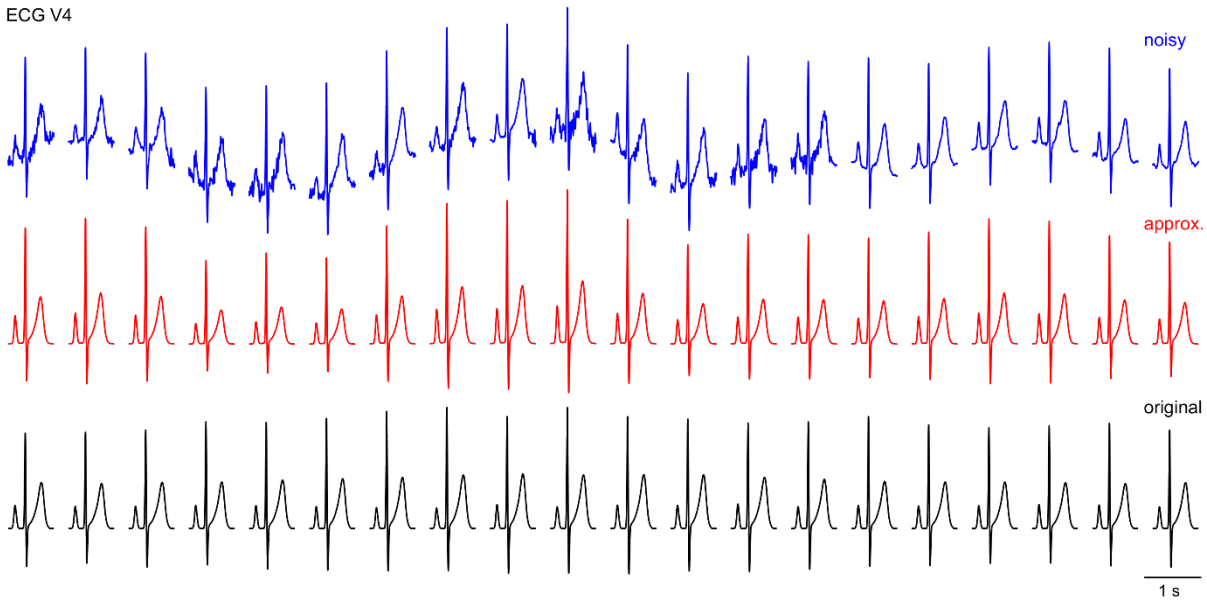

Figure 6. Denoising of simulated 12-lead ECG. Shown are 20 consecutive out of 1,000 segments of Wilson lead V4, each containing P-wave, QRS-complex and T-wave. The original signal segments are shown in black, the noisy signal segments in blue, and the approximated or denoised signal segments in red. Observe that the amplitudes of the P-waves, QRS-complexes, and T-waves of the denoised segments are coupled in some way to the low-frequency component present in the noisy segments. On the other hand, it is clear that higher-frequency noise or artifacts have been removed excellently. The overall signal-to-noise ratio is $\sigma_S/\sigma_N = 0.5$.

4. DISCUSSION AND CONCLUSIONS

A method for compression and denoising multichannel ECG signals was presented. The method is based on the third-order tensor decomposition, i.e., third-order SVD. The first main step of the method is QRS-aligned signal segmentation, which results in a three-dimensional data structure, the dimensions being time, channel, and segment (heartbeat epoch). This three-dimensional array was considered a third-order tensor, opening the possibility of a tensor decomposition. The third-order SVD was chosen as the decomposition method. Appropriate components of the structures into which the tensor was decomposed were then selected for further processing. The resulting approximation can be used both for lossy data compression and for noise reduction.

The performance of the method was demonstrated using a 12-lead ECG. The results obtained for original signals and original signals contaminated with Gaussian white noise show that the method can achieve both strong compression and excellent noise reduction. In particular, the time courses of the P-waves, QRS-complexes and T-waves are hardly affected despite strong compression and noise removal.

The comparison with the single-channel SVD-based noise reduction clearly showed the superiority of the tensor-based method. The reason for this advantage of the proposed method is that it can use correlations within all individual channels and between all channels of multichannel time series in order to compress the signals and to separate the wanted signal and noise. This finding is consistent with the results reported for multichannel singular spectrum analysis based on denoising multichannel signals (Schanze, 2023a; Schanze, 2023b). A similar result was found in the denoising of multichannel signals using autoencoders (Saman & Schanze, 2023).

Two problems that have been encountered with tensor-based denoising are the choice of the components useful for approximation or denoising and the signal-noise coupling of some of these components. A possible solution to the first problem is a more detailed analysis of the components created by the decomposition. The second problem is probably more difficult, especially when the desired signal and noise are coupled.

Due to its construction, the third-order SVD is multilinear. Thus, non-linear interactions in the multichannel signal to be processed, e.g., denoised, may not be exploited.

It is obvious that due to the high dimensionality of a lot of many data sets, tensor decompositions require suitable and fast computer algorithms (Bader et al., 2022; Kolda & Bader, 2009). Despite the costs involved, it is often advantageous to analyse and process higher-dimensional data using higher-dimensional methods, as has also been shown in this work.

To conclude, the proposed method could be a useful tool for biomedical signal processing. Especially with regard to the goal that compression and denoising methods should remove redundant or unwanted components of a measured signal, but at the same time leave the actual useful or wanted components of the signal unchanged.

However, a rigorous, and of course, statistical analysis of the methods presented, the comparison with other methods, e.g., classical linear filtering or recently developed machine learning approaches (e.g., Samann & Schanze, 2023), the use of better signal and noise models, also in conjunction with cross-channel correlations, such as in the case of Einthoven's law, and the development and testing of methods for the selection of the components obtained by tensor decomposition of the tensorized data for effective compression and efficient denoising are tasks for future work. The same applies to testing the presented methods in the real world, e.g. in clinical applications.

Acknowledgments

The author thanks Fars Samann and Tobias Ott for discussions.

References

1. AlGhatrif, M., Lindsay, J. (2012) A brief review: history to understand fundamentals of electrocardiography. *J. Community Hosp. Intern. Med. Perspect.*, 2(1), DOI: 10.3402/jchimp.v2i1.14383.
2. Andrews, H., Patterson, C. (1976) Singular value decompositions and digital image processing. *IEEE Transactions on Acoustics, Speech, and Signal Processing*, 24(1), 26-53, DOI: 10.1109/TASSP.1976.1162766.
3. Ardeti, V. A., Kolluru, V. R., Varghese, G. T., Patjoshi, R. K. (2023) An overview on state-of-the-art electrocardiogram signal processing methods: Traditional to AI-based approaches. *Expert Systems with Applications*, 217, 119561.
4. Bader, B. W., Kolda, T. G., et al. (2022) Tensor toolbox for MATLAB, Version 3.4, www.tensortoolbox.org.
5. Chatterjee, S., Thakur, R. S., Yadav, R. M., Gupta, L., Raghuvanshi, D. K. (2020) Review of noise removal techniques in ECG signals. *IET Signal Processing*, 14, 569-590.
6. Elgendi, M., Mohamed, A., Ward, R. (2017) Efficient ECG compression and QRS detection for e-health applications. *Sci. Rep.*, 7, 459, https://doi.org/10.1038/s41598-017-00540-x.
7. Fan, L., Zhang, F., Fan, H., Zhang, C. (2019) Brief review of image denoising techniques. *Vis. Comput. Ind. Biomed. Art*, 2, 1-12.
8. Fye, W. B. (1994) A history of the origin, evolution, and impact of electrocardiography. *Am. J. Cardiol.*, 73(13), 93749.
9. Golyandina, N., Zhigljavsky, A. (2020) *Singular spectrum analysis for time series*. 2nd ed. Berlin: Springer-Verlag.
10. Golub, G. H., Reinsch, C. (1970) Singular value decomposition and least squares solutions. *Numer. Math.*, 14, 403-420, https://doi.org/10.1007/BF02163027.
11. Gong, W., Li, H., Zhao, D. (2017) An improved denoising model based on the analysis K-SVD algorithm. *Circuits Syst. Signal Process.*, 36, 4006-402, https://doi.org/10.1007/s00034-017-0496-7.
12. Halidou, A., Mohamadou, Y., Ari, A. A. A. et al. (2023) Review of wavelet denoising algorithms. *Multimed. Tools. Appl.*, https://doi.org/10.1007/s11042-023-15127-0.
13. Howell, J. D. (1991) Diagnostic technologies - X-rays, electrocardiograms, and cat-scans. *South. Calif. Law Rev.*, 65(1), 529-564.
14. Limaye, H., Deshmukh, V. V. (2016) ECG noise sources and various noise removal techniques: A survey. *International Journal of Application or Innovation in Engineering & Management*, 5(2), 86-92.
15. Kher, R. (2019) Signal processing techniques for removing noise from ECG signals. *J. Biomed. Eng.*, 1, 1-9.
16. Kolda, T. G, Bader, Brett W. (2009) Tensor decompositions and applications. *SIAM Review*, 51(3), 455-500.
17. Jain, A. K. (1981) Image data compression: A review. *Proceedings of the Institute of Electrical and Electronics Engineers (IEEE)*, 69, 349-389, https://doi.org/10.1109/PROC.1981.11971.
18. Jalaleddine, S. M. S., Hutchens, C. G., Strattan, R. D., Coberly, W. A. (1990) ECG data compression techniques-a unified approach. *IEEE Transactions on Biomedical Engineering*, 37(4), 329-343.
19. Jayasankar, U., Thirumal, V., Ponnurangam, D. (2021) A survey on data compression techniques: From the perspective of data quality, coding schemes, data type and applications. *Journal of King Saud University – Computer and Information Sciences*, 33, 119-140.
20. Liu, F. F, Liu, C. Y., Zhao, L. N., Zhang, X. Y., Wu, X. L., Xu, X. Y., et al. (2018) An open access

database for evaluating the algorithms of ECG rhythm and morphology abnormal detection. *Journal of Medical Imaging and Health Informatics*, 8, 1368-1373.
21. Liu, Y. (ed.) (2021) *Tensors for Data Processing*. Academic Press.
22. Maghfiroh, A. M. et al. (2022) State-of-the-art method denoising electrocardiogram signal: A review. In: Triwiyanto, T., Rizal, A., Caesarendra, W. (eds.) Proceedings of the 2nd International Conference on Electronics, Biomedical Engineering, and Health Informatics. *Lecture Notes in Electrical Engineering, 898*. Springer, Singapore. https://doi.org/10.1007/978-981-19-1804-9_24.
23. *Mac Duffee, C. C. (1933) The Theory of Matrices. Ergebnisse der Mathematik und Ihrer Grenzgebiete, 5. Springer, Berlin, Heidelberg. https://doi.org/10.1007/978-3-642-99234-6_4.*
24. *Ouali, M. A., Chafaa, K. (2013) SVD-based method for ECG denoising. 2013 International Conference on Computer Applications Technology (ICCAT), Sousse, Tunisia, 2013, 1-4, DOI: 10.1109/ICCAT.2013.6522051.*
25. *Salomon, D. (2007) Data Compression. Springer Verlag London.*
26. *Sanei, S., Hassani, H. (2016) Singular spectrum analysis for biomedical signals. 2nd ed., Boca Raton: CRC Press.*
27. *Samann, F., Schanze, T. (2021) Denoising biomedical signals via adaptive low-rank matrix representation by singular value decomposition using wavelets. 4th Intern. Conf. on Bio-Engineering for Smart Technol., Paris/Créteil, France, 1-4, DOI: 10.1109/BioSMART54244.2021.9677889.*
28. *Samann, F., Schanze, T. (2023) Multiple ECG segments denoising autoencoder model. Biomedical Engineering / Biomedizinische Technik, https://doi.org/10.1515/bmt-2022-0199.*
29. *Schanze, T. (2018) Compression and noise reduction of biomedical signals by singular value decomposition. IFAC-PapersOnLine, 51, 361-366.*
30. *Schanze, T. (2022) On the use of singular value decomposition for QRS detection and ECG denoising. Current Directions in Biomedical Engineering, 8(2), 77-80.*
31. *Schanze T. (2023a) Tensor-based approximation of multichannel ECG sections. Proc AUTOMED 2023, ID741, https://doi.org/10.18416/AUTOMED.2023.*
32. *Schanze T. (2023b) Third-order SVD based denoising of multichannel ECG. Accepted: Current Directions of Biomedical Engineering.*
33. *Sološenko, A., Petrėnas, A., Paliakaitė, B., Marozas, V., & Sörnmo, L. (2021) Model for simulating ECG and PPG signals with arrhythmia episodes (version 1.3.0). PhysioNet, https://doi.org/10.13026/c5qq-2g72.*
34. *Stewart, G. W. (1993) On the early history of the singular value decomposition. SIAM Review, 35(4), 551-566.*
35. *Wei, J.-J., Chang, C.-J., Chou, N.-K., Jan, G.-J. (2001) ECG data compression using truncated singular value decomposition. IEEE Transactions on Information Technology in Biomedicine, 5(4), 290-299, DOI: 10.1109/4233.966104.*
36. *Wrede, R. C. (1972) Introduction to Vector and Tensor Analysis.* Dover Publications Inc.